Evidence for necrosis, but not apoptosis, in human hepatoma cells with knockdown of mitochondrial aquaporin-8

Maria J. Marchissio, Daniel E. A. Francés, Cristina E. Carnovale & Raúl A. Marinelli

Apoptosis
An International Journal on Programmed Cell Death

ISSN 1360-8185

Apoptosis
DOI 10.1007/s10495-014-0966-3

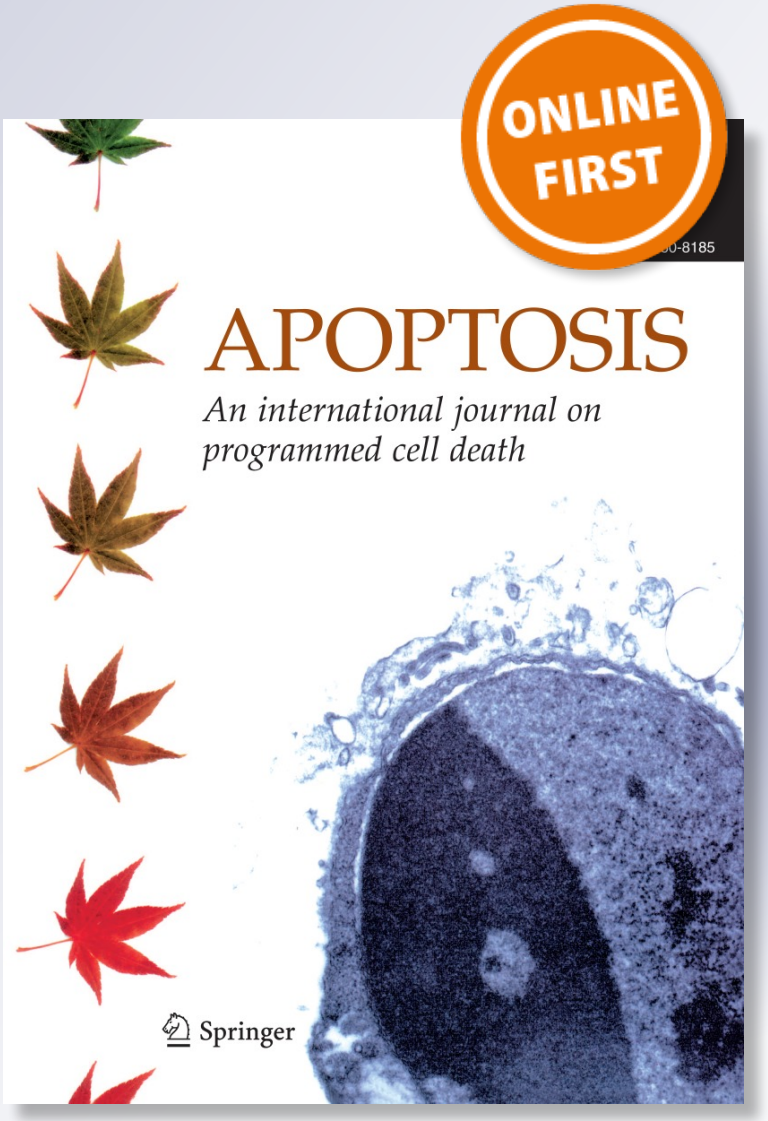

Springer

Apoptosis
DOI 10.1007/s10495-014-0966-3

ORIGINAL PAPER

Evidence for necrosis, but not apoptosis, in human hepatoma cells with knockdown of mitochondrial aquaporin-8

Maria J. Marchissio · Daniel E. A. Francés · Cristina E. Carnovale · Raúl A. Marinelli

Abstract We previously found that mitochondrial aquaporin-8 (mtAQP8) channels facilitate mitochondrial H_2O_2 release in human hepatoma HepG2 cells and that their knockdown causes oxidant-induced mitochondrial dysfunction and loss of viability. Here, we studied whether apoptosis or necrosis is involved as the mode of cell death. We confirmed that siRNA-induced mtAQP8 knockdown significantly decreased HepG2 viability by MTT assay, LDH leakage, and trypan blue exclusion test. Analysis of mitochondrial proapoptotic Bax-to-antiapoptotic Bcl_{XL} ratio, mitochondrial cytochrome c release and caspase-3 activation showed no alterations in mtAQP8-knockdown cells. This indicates a primary mechanism of cell death other than the intrinsic mitochondrial apoptotic pathway. Thus, nuclear staining with DAPI did not reveal any increase of apoptotic features, i.e. chromatin condensation or nuclear fragmentation. Flow cytometry studies after double cell staining with annexin V and propidium iodide confirmed lack of apoptosis and suggested necrosis as the primary mechanism of death in mtAQP8-knockdown HepG2 cells. Necrosis was further supported by the increased nuclear delocalization and extracellular release of the High Mobility Group Box 1 protein. The knockdown of mtAQP8 in another human hepatoma-derived cell line, i.e. HuH-7 cells, also induced necrotic but not apoptotic death. Our data suggest that mtAQP8 knockdown induces necrotic cell death in human neoplastic hepatic cells, a finding that might be relevant to therapeutic strategies against hepatoma cells.

Keywords Aquaporin-8 · Mitochondria · Apoptosis · Necrosis · HepG2 · HuH-7

Abbreviations

AQP	Aquaporin
AQP8	Aquaporin-8
mtAQP8	Mitochondrial aquaporin-8
H_2O_2	Hydrogen peroxide
ROS	Reactive oxygen species
siRNA	Short interfering RNA
SCR	Scrambled $siRNA_1$ sequence
IMM	Inner mitochondrial membranes
OTC	Ornithine transcarbamylase
DAPI	4′,6-Diamidino-2-phenylindole
PI	Propidium iodide
MTT	3-(4,5-Dimethyl-2-yl)-2,5-diphenyltetrazolium bromide
LDH	Lactate dehydrogenase

Introduction

Aquaporin-8 (AQP8), a member of the mammalian AQP family of channel proteins, was found to facilitate the transmembrane diffusion of H_2O_2 using reconstituted yeast [1] and transfected mammalian cells [2]. AQP8 is expressed in the inner mitochondrial membranes of rodent hepatocytes [3, 4] and human hepatocarcinoma-derived HepG2 cells [5].

We recently provided experimental evidence suggesting that in HepG2 cells, mitochondrial AQP8 (mtAQP8)

M. J. Marchissio · D. E. A. Francés · C. E. Carnovale · R. A. Marinelli (✉)
Instituto de Fisiología Experimental, Facultad de Ciencias Bioquímicas y Farmacéuticas, Consejo Nacional de Investigaciones Científicas y Técnicas (CONICET), Universidad Nacional de Rosario, Suipacha 570, 2000 Rosario, Santa Fe, Argentina
e-mail: rmarinel@unr.edu.ar; marinelli@ifise-conicet.gov.ar

Published online: 12 January 2014

facilitates the mitochondrial release of H_2O_2 and that mtAQP8 knockdown causes ROS-induced mitochondrial depolarization via the mitochondrial permeability transition mechanism [5]. As the oxidant-induced mitochondrial dysfunction led to loss of viability in mtAQP8-knockdown HepG2 cells, we now explored whether an apoptotic pathway was activated as the mechanism of cell death. Our results suggest that the primary mechanism of death in human hepatoma cells with mtAQP8 knockdown is not apoptosis but necrosis.

Materials and methods

Materials and reagents

Dulbecco's Modified Eagle Medium, L-glutamine, Pen-Strep antibiotic mixture, 0.25 % Trypsin–EDTA and Lipofectamine 2000 Reagent were all from Invitrogen Corp., CA, USA. Non-essential amino acids and Foetal Calf Serum were purchased from PAA Laboratories GmbH, Linz, Austria. Silencer siRNA Construction kit was from Ambion, TX, USA. EnzCheck Caspase-3 assay kit 1, and ProLong+DAPI were obtained from Molecular Probes, OR, USA. Anti-HMGB-1, Bax, Bcl_{XL}, Cytochrome c and Caspase-3 antibodies were all from Santa Cruz Biotechnology Inc., CA, USA, whilst anti-prohibitin was from Abcam, Cambridge, UK and anti-β-actin from Sigma, MO, USA as well as the protease inhibitors Phenyl-methylsulfonyl fluoride and Leupeptin, and Cy3 secondary antibody. Sucrose was purchased from Merck Chemicals, Darmstadt, Germany. Materials for immunoblotting were obtained as follows: Polyscreen PVDF transfer membrane from Perkin Elmer Life and Analytical Sciences, MA, USA; Pierce ECL Western Blotting Substrate from Thermo Scientific, IL, USA; and Kodak XAR film from Eastman Kodak, NY, USA

Cell culture and incubation

HepG2 clone C3A (ATCC CRL-10741) and HuH-7 (ATCC) cells were cultured in T75 flasks in Dulbecco's Modified Eagle Medium (4.5 g/l, high glucose formulation), supplemented with 2 mM L-glutamine, 0.1 mM non-essential amino acids, 10 % heat-inactivated foetal calf serum and 100 I.U. penicillin/100 μg streptomycin at 37 °C in a 5 % CO_2 atmosphere. Media was changed every other day and cells were trypsinized after reaching confluency.

Synthesis of short interfering RNA (siRNA) and AQP8 knockdown

As we previously reported [5], the 21-nucleotide RNA duplexes were synthesized using the Silencer siRNA kit following the manufacturer's directions, with oligonucleotides synthesized by Invitrogen as templates. Two target sequences were chosen following the guidelines described by Elbashir et al. [6], and they induced a significant decrease in AQP8 expression, as analyzed by immunoblotting. $siRNA_1$ was specifically targeted to nucleotides 177–197 (AACGG TTTGTGCAGCCATGTC) and $siRNA_2$ to nucleotides 749–769 (AACCACTGGAACTTCCACTGG) of human AQP8. The control siRNA (SCR) was designed by randomly scrambling the nucleotides of $siRNA_1$ (AATGTGTCCGT-GAGCACGTCT). mtAQP8 protein expression was analyzed in the cells 72 h afterward by immunoblotting.

Subcellular fractionation

Cells were harvested in 0.3 M sucrose, sonicated, and subjected to low-speed centrifugation to obtain postnuclear supernatants which were then centrifuged at 6,200×*g* for 10 min, yielding the mitochondrial and cytoplasmic fractions.

Mitochondria were washed twice before being resuspended in the appropriate buffers or were used to obtain HuH-7 inner mitochondrial membranes (IMM), as described by Ragan et al. [7]. First, mitoplasts were prepared by using the detergent approach. Briefly, digitonin was added to a suspension of mitochondria (100 mg of protein/ml) to a final concentration of 0.6 % w/v in 0.3 M sucrose and incubated for 15 min on ice under gentle stirring. After dilution with 3 volumes of 0.3 M sucrose, the suspension was centrifuged at 15,000×*g* for 10 min at 4 °C. The resulting pellet (mitoplasts) was resuspended in isolation medium at a protein concentration of 15 mg/ml before being sonicated. Mitoplasts were then diluted with an equal volume of 0.3 M sucrose and centrifuged at 15,000×*g* for 10 min at 4 °C. The resulting pellet was resuspended in 10 volumes of 0.3 M sucrose and centrifuged again at 100,000×*g*; this process was repeated twice. The final pellet (i.e., IMM) was resuspended in 0.3 M sucrose with protease inhibitors.

Additionally, HepG2 cells were only sonicated to obtain the whole lysate fraction. Protein content was determined according to Lowry et al. [8].

Immunoblotting

The different cell extracts were prepared as described above and heated 15 min at 90 °C in sample buffer (20 mM Tris, pH 8.5, 1 % SDS, 400 μM DTT, 10 % glycerol), subjected to 12 % SDS-PAGE and transferred to polyvinyl difluoride membranes. After blocking for a minimum of 2 h and washing, blots were incubated overnight at 4 °C with goat antibodies against caspase-3 (0.7 μg/ml) or human AQP8 (1 μg/ml), mouse affinity-purified antibodies against Bcl_{XL} (0.7 μg/ml), Bax (0.7 μg/

ml), Cytochrome c (0.3 μg/ml), or Ornithine Transcarbamylase (0.7 μg/ml). As loading controls, membranes were also incubated with rabbit antibodies against Prohibitin (0.1 μg/ml), or with a monoclonal antibody against β-actin (0.3 μg/ml). The blots were then washed extensively and incubated with the horseradish peroxidase-conjugated corresponding secondary antibodies; bands were detected by the enhanced chemiluminescence detection system (ECL) and autoradiographs were obtained by exposing PVDF membranes to radiographic film. Densitometric analysis of the developed bands was performed using ImageJ Software by Rasband [9].

Fluorometric analysis of caspase-3 activity

72 h after transfection, HepG2 cells were harvested by scraping from the dishes, washed with ice-cold PBS, and resuspended in 0.3 M sucrose and sonicated. After centrifugation at 16,000×*g* for 5 min at 4 °C, supernatants were assessed for caspase-3 activity using the EnzCheck Caspase-3 assay kit by following the manufacturer's instructions. The reaction is based on the proteolytic cleavage of the weakly fluorescent 7-amino-4-methylcoumarin-derived substrate Z-DEVD–AMC, which yields a bright blue–fluorescent product. Fluorescence was determined using a fluorescence microplate reader (Beckman Coulter DTX 880 Multimode Detector) set at an excitation wavelength of 355 nm and an emission wavelength of 460 nm.

4′,6-Diamidino-2-phenylindole (DAPI) staining for nuclear condensation and fragmentation

HepG2 cells were transfected with siRNAs and after 72 h, they were fixed with 4 % paraformaldehyde on slide glasses for 30 min at room temperature. The fixed cells were washed with PBS and permeabilized and blocked with 0.2 % Triton X-100/BSA 3 % for 10 min. After washing, nuclei were stained with ProLong+DAPI. Fluorescence localization was detected by confocal microscopy in a Nikon C1SiR with inverted microscope Nikon TE200 equipment. Images were collected with equal confocal settings in each particular set of experiments. Under the same settings, no autofluorescence was detected. Apoptotic cells, if present, were identified by nuclear condensation and fragmentation.

Annexin V-FITC/PI staining assay

Cellular death mechanism was determined by staining cells with annexin V conjugated with fluorescein isothiocyanate (FITC) and propidium iodide (PI) labeling. Annexin V can identify externalization of phosphatidylserine during the progression of apoptosis, and therefore can detect cells in early stages of apoptosis, whilst PI can label the cellular DNA in necrotic cells where the cell membrane has been totally compromised.

To this purpose, at 72 h post-transfection, HepG2 and HuH-7 cells were collected, washed and stained with annexin V-FITC and propidium iodide by use of the Annexin V-FITC Apoptosis Detection Kit coupled to flow cytometric analysis (Cell Sorter BD FACSAria II, Becton, Dickinson and Co, Franklin Lakes, NJ), following the manufacturer's instructions. Briefly, cells were trypsinized, washed twice with cold PBS and then re-suspended in 500 μl binding buffer, prior to incubation with annexin V-FITC and PI in the dark for 15 min at room temperature. Detection of green and red fluorescence was performed, and the proportion of annexin V and PI positive cells were determined in the indicated experimental groups. Green and red fluorescence intensities detected in non stained cells were used to set the thresholds for each channel. Viable cells were negative for both PI and annexin V and apoptotic cells were positive for annexin V and negative for PI, while late apoptotic dead cells displayed both high annexin V and PI labeling. Non-viable cells, which underwent necrosis, were positive for PI and negative for annexin V.

Cellular viability measurements

MTT assay

The effect of mtAQP8 knockdown on mitochondrial activity was estimated 72 h post-transfection by use of the MTT assay with the Cell Titer 96 Nonradioactive cell proliferation assay kit, as previously reported by us [5]. The absorbance of the reaction was recorded at 570 nm with a Perkin Elmer Lambda XLS+spectrophotometer.

LDH assay

Lactate dehydrogenase activity was used as a measure of cell viability as we previously reported [5] by measuring the enzyme's leakage with the LDH assay kit 72 h after transfection. The percentage of LDH release was determined by dividing the LDH released into the media by the total LDH (released plus cellular). Cellular LDH samples were obtained by lysis of the same cells by sonication. Absorbance at 340 nm was recorded using a microplate analysis spectrometer (Beckman Coulter DTX 880 Multimode Detector).

Trypan blue exclusion assay

At 72 h after transfection, cells were trypsinized and an aliquot of collected cells was combined with trypan blue dye and analyzed microscopically on a Neubauer counting chamber. Blue cells were counted as nonviable, and cells

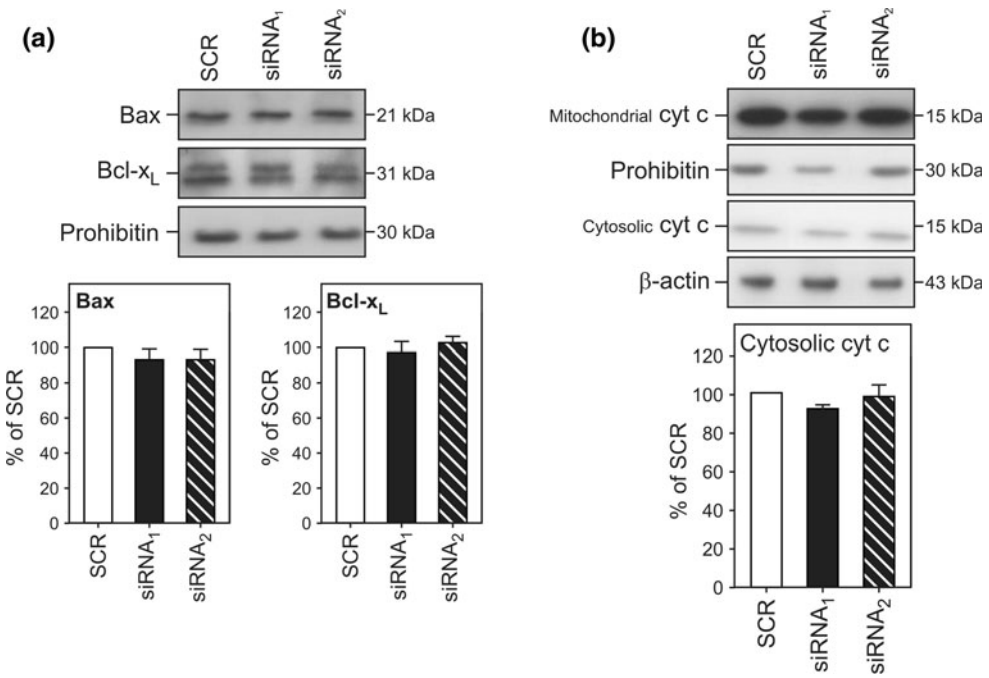

Fig. 1 No activation of the mitochondrial apoptotic pathway in mtAQP8-knockdown HepG2 cells. HepG2 cells were transfected with siRNA1, siRNA2 or a scrambled siRNA1 sequence (SCR) for 72 h and then, proteins involved in activation of the mitochondrial apoptotic pathway of cell death were assessed. **a** Expression of Bax and Bcl-x_L in mitochondrial fractions along with the corresponding densitometric analysis. **b** Expression of mitochondrial, and cytosolic cytochrome c with densitometric analysis. Data are mean ± s.e.m. of three independent experiments. Prohibitin (mitochondrial fraction) and β-actin (cytosolic fraction) were used as loading controls

excluding the dye were counted as viable. Cell viability was expressed as percentage of viable cells as we previously report [5].

Fluorescence immunostaining for HMGB-1

HepG2 cells were cultured on glass cover slips and transfected with the different siRNAs. 73 h post-transfection, cells were fixed with 4 % formaldehyde for 10 min, and permeabilized with 0.2 % Triton X-100 in PBS containing 0.2 % BSA. After extensive washing with PBS cells were sequentially incubated with mouse anti-HMGB-1 antibodies and anti-mouse secondary antibodies conjugated with cyanine 3, and subsequently mounted with ProLong+DAPI. Fluorescence images were captured by confocal microscopy (Nikon C1SiR with a Nikon TE200 inverted microscope). Under these conditions, no autofluorescence was detected, nor was it evidenced in the controls carried out by omission of primary or secondary antibodies.

HMGB-1 nuclear delocalization was estimated as the number of nuclei with fading fluorescence associated with increased cytoplasmic (perinuclear) fluorescence.

HMGB-1 Western blotting analysis

72 h after transfection, extracellular medium from $siRNA_1$, $siRNA_2$ and SCR-transfected HepG2 cells was harvested and spun at 500×*g* for 5 min. Supernatants were then filtered through 0.45 µm membranes to remove cell debris and macromolecular complexes. Samples were then concentrated with 10 % TCA and proteins in the concentrated cell culture supernatants were subjected to immunoblotting with primary antibodies specific for HMGB-1.

Statistical analysis

Data are expressed as mean ± s.e.m. and as percentage of the controls (i.e., SCR). Significance was determined using one-way ANOVA, followed by Tukey test. $p < 0.05$ was considered as statistically significant.

Results

No activation of the mitochondrial apoptotic pathway in mtAQP8-knockdown HepG2 cells

In order to begin studying the mechanisms of death in HepG2 cells with mtAQP8-knockdown, we evaluated the activation of the intrinsic mitochondrial apoptotic pathway. As shown in Fig. 1a, there was no significant change in mitochondrial levels of proapoptotic (i.e., Bax) or antiapoptotic (i.e., Bcl_{XL}) proteins or in the mitochondrial Bax-to-Bcl_{XL} ratio (0.98 ± 0.30 for $siRNA_1$ and 1.05 ± 0.04

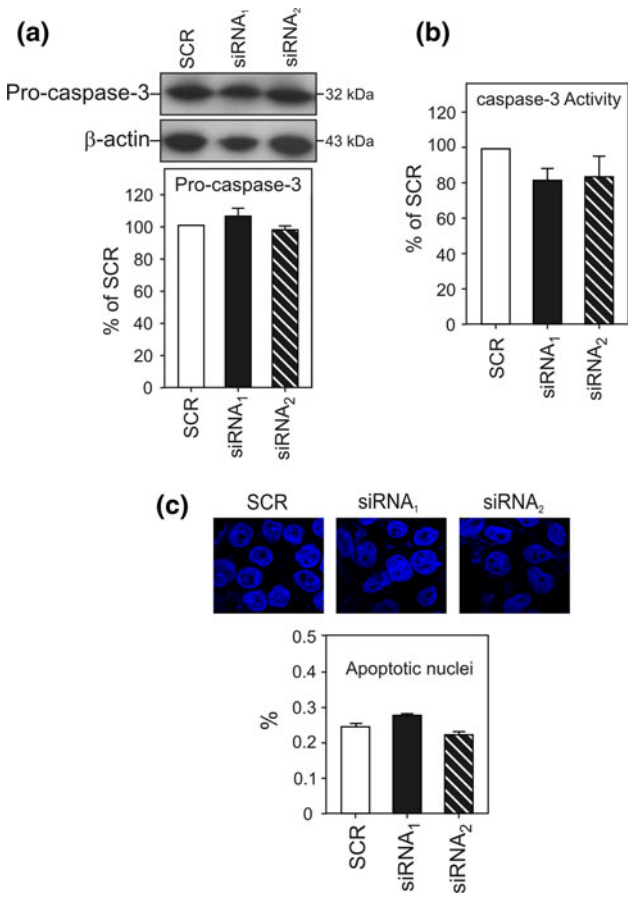

Fig. 2 No activation of caspase-3 in HepG2 cells with mtAQP8-knockdown. HepG2 cells were transfected with siRNA1, siRNA2 or a scrambled siRNA1 sequence (SCR) for 72 h and then, caspase 3 activation and activity were assessed. **a** Expression of pro-caspase-3 with densitometric analysis. **b** Caspase 3/caspase 3-like activity. Data are mean ± s.e.m. of three independent experiments. β-actin (cytosolic fraction) were used as loading controls. **c** HepG2 cells were transfected with either siRNA1, siRNA2 or SCR for 72 h, stained with DAPI and then, changes in nuclear morphology were determined by confocal fluorescence microscopy

for $siRNA_2$, considering SCR ratio as 1.00). Similarly, mitochondrial cytochrome c was not released into the cytoplasm (Fig. 1b).

There was no activation of caspase-3, detected by two different methods. Firstly, since the caspase-3 antibody used for Western blotting did not efficiently detect the active 17 kDa subunit, its activation was evaluated by this method based on the disappearance of its 32 kDa precursor form, which did not diminish with the siRNA treatment (Fig. 2a), showing that there was no cleavage of pro-caspase-3 throughout the whole period of mtAQP8 knockdown. Also, as shown in Fig. 2b, caspase 3/caspase 3-like enzymatic activity was assessed and no changes were observed in it ($siRNA_1$: 82 ± 6 %; $siRNA_2$: 84 ± 11 %; data are presented as arbitrary fluorescence units per mg of protein, expressed as percentage of SCR and represent mean ± s.e.m. of three independent experiments). The absence of activation of the apoptotic effector caspase-3 does not favor apoptosis as a mechanism for death in mtAQP8-knockdown HepG2 cells.

Cell morphology was also assessed by DAPI staining. As shown in Fig. 2c, the nuclear structure of mtAQP8-knockdown cells remained intact, with no chromatin condensation or apoptotic body formation characteristic of apoptosis observed.

Together, these data suggest a primary mechanism of death in mtAQP8-knockdown HepG2 cells other than apoptosis.

Evidence for necrosis in mtAQP8-knockdown HepG2 cells

The type of cell death, apoptosis or necrosis, caused by mtAQP8-knockdown was evaluated in HepG2 cells by flow cytometry after double staining with annexin V and PI.

As shown in Fig. 3a, viable cells appear on the annexin V (−) PI (−) (lower left quadrant) field. mtAQP8-knockdown induced an important increase in PI fluorescence as evidenced by the population in the annexin V (−) PI (+) (upper left quadrant) field indicative of necrosis. The percentage of events in each quadrant is shown in Fig. 3b. Thus, necrosis seems to be the primary mechanism of death in mtAQP8-knockdown HepG2 cells.

We extended our studies on the cell death mechanism by analyzing High Mobility Group Box 1 (HMGB-1), a non-histone nuclear protein ubiquitously expressed in eukaryotes that plays an important role in the regulation of gene transcription within the nucleus [10]. Upon release by phagocytes and damaged/necrotic cells [11], extracellular HMGB-1 contributes to the pathogenesis of various inflammatory diseases and is considered a marker for necrosis since in apoptotic cells, most of HMGB-1 binds to the condensed nuclear chromatin [12].

Following immunostaining, HMGB-1 was found predominantly in the nucleus of control HepG2 cells. However, we found a significant increase in nuclear delocalization of HMGB-1 induced by siRNA treatment, i.e., nuclear fluorescence fading and appearance of cytoplasmic (perinuclear) fluorescence (Fig. 4a). Consistently, we observed an increase in the extracellular release of HMGB-1 (Fig. 4b).

Viability of HuH-7 with mtAQP8-knockdown

We first confirmed the expression of AQP8 in IMM of HuH-7 cells as previously shown for HepG2 cells [5], i.e., by mitochondrial subfractionation and immunoblotting studies using a commercially available affinity-purified antibody raised

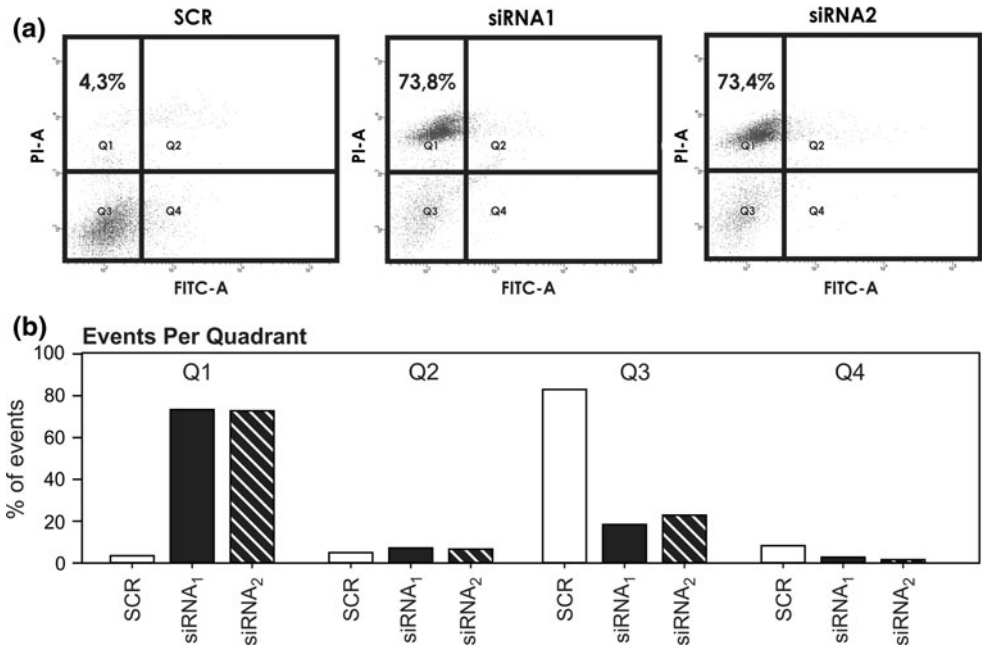

Fig. 3 Assessment of cell death by flow cytometry. mtAQP8 knockdown HepG2 cells were stained with annexin V-FITC and PI, and then analyzed by flow cytometry as described under Materials and methods. **a** Lower left quadrant (Q3) represents viable cells (annexin V-negative/PI-negative), upper left quadrant (Q1), necrotic cells (annexin V-negative/PI-positive), lower right quadrant (Q4), early apoptosis cells (annexin V-positive/PI-negative) cells; upper right quadrant (Q2), late-apoptotic cells (annexin V-positive/PI-positive). The analysis shows an increase in the necrotic cell population from 4 to 72–74 % with the mtAQP8 knockdown. The figure is representative of three experiments with similar results. **b** *Bars* represent the percentage of events in each quadrant

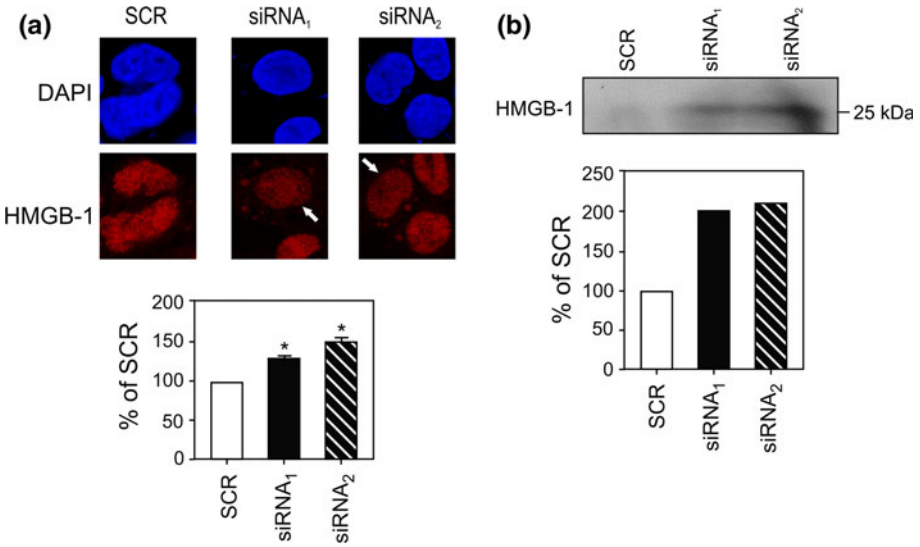

Fig. 4 Effects of mtQAP8 knockdown on nuclear delocalization and release of HMGB-1 in HepG2 cells. **a** Confocal immunofluorescence microscopy for HMGB-1 in HepG2 cells with mtAQP8 knockdown. Nuclear DAPI staining is in *blue*. Nuclear delocalization, estimated as the number of nuclei with fading fluorescence associated with cytoplasmic (perinuclear) fluorescence is expressed as percentage of SCR. Data are mean ± s.e.m. of about 300 cells per group. $*p < 0.05$ versus SCR. **b** HMGB-1 immunoblotting analysis in extracellular media of HepG2 cells at 72 h post-transfection with siRNA. HMGB-1 levels were determined by the relative optical intensity of the immunoreactive bands, and expressed as % of SCR. Data are representative of two independent experiments

against human AQP8. Mitochondrial subfractionation showed a band of expected size (28 kDa) that was enriched in highly purified IMM (Fig. 5a). Moreover, the specificity of the AQP8 immunoblot was verified by the decrease of the intensity of the immunodetected band in samples from AQP8-knockdown cells (Fig. 4b, see below for explanation).

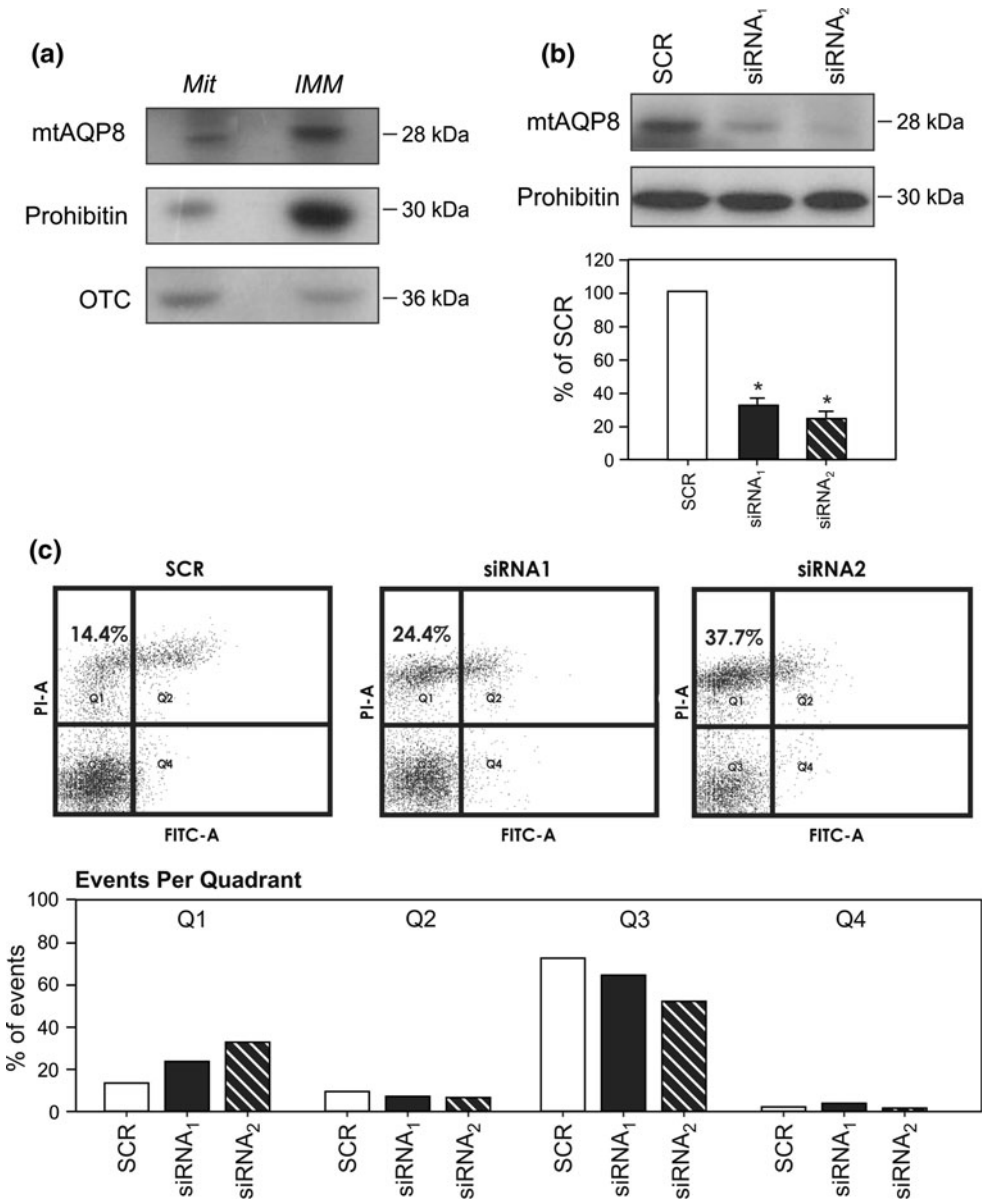

Fig. 5 Expression and knockdown of mtAQP8 in HuH-7 cells, and assessment of cell death by flow cytometry. **a** Immunoblotting for AQP8 in mitochondrial (Mit) and inner mitochondrial membrane (IMM) fractions in HuH-7 cells. Each lane was loaded with 20 μg of protein. Bands migrated approximately to 28 kDa, and showed enrichment from Mit to IMM. Immunoblottings were reprobed for prohibitin (IMM marker) and OTC (ornithine transcarbamylase, matrix protein) as controls. **b** Representative immunoblotting for mtAQP8 in mitochondrial fractions of HuH-7 cells at 72 h post-transfection, and corresponding densitometric analysis related to prohibitin. Each lane was loaded with 20 μg of protein. Data are presented as percentages of SCR and represent mean ± s.e.m. of three independent experiments. $*p < 0.05$ from SCR. **c** mtAQP8 knockdown HuH-7 cells were stained with annexin V-FITC and PI, and then analyzed by flow cytometry as described under Materials and Methods. The analysis shows an increase in the necrotic cell population from 14 to 30 % with the mtAQP8 knockdown. The figure is representative of three experiments with similar results and includes dot-plot quadrants and *bars* representing the percentage of events in each quadrant

To induce a decrease in mtAQP8 expression, HuH-7 cells were then transfected with siRNAs specific for human AQP8. As observed for HepG2 [5], mtAQP8 protein was significantly knocked down at 72 h. Densitometric analysis of mtAQP8 levels related to prohibitin (an IMM protein) indicated a decrease in mtAQP8 expression of around 70 %.

As we previously reported [5] and is shown in Table 1, mtAQP8-knockdown HepG2 cells displayed a reduced viability. mtAQP8 knockdown in HuH-7 cells also induced loss of viability.

Similarly to that shown in Fig. 3 for HepG2 cells, flow cytometry studies in mtAQP8-knockdown HuH-7 cells

Table 1 Cell viability assays in mtAQP8-knockdown cells

	MTT (% of SCR)	LDH (% of total LDH)	Trypan blue (% of cell viability)
HepG2			
SCR	100 ± 0	5.2 ± 0.4	94 ± 2
$siRNA_1$	51 ± 8*	10.4 ± 2.7*	64 ± 8*
$siRNA_2$	58 ± 7*	11.6 ± 2.5*	61 ± 7*
HUH-7			
SCR	100 ± 0	5.2 ± 0.3	98 ± 0
$siRNA_1$	84 ± 1*	6.5 ± 0.2*	87 ± 1*
$siRNA_2$	83 ± 1*	7.0 ± 0.2*	86 ± 1*

Cells were transfected with specific siRNAs or scrambled siRNA sequence (SCR) as indicated in Materials and methods and then, the viability was assessed

Data are mean ± s.e.m. of 3–4 independent experiments

* $p < 0.05$ versus SCR

indicated necrosis but not apoptosis as the mode of cell death. Thus, the percentage of cells displaying PI fluorescence (upper left quadrant, Q1) was increased up to 24 and 38 % for siRNA1 and siRNA2, respectively. Percentages of events in quadrants Q2 and Q4, indicative of apoptosis, were unaltered.

Discussion

Recently, we reported that the knockdown of mtAQP8 expression in HepG2 cells impairs mitochondrial H_2O_2 release and increases mitochondrial ROS. This caused ROS-induced mitochondrial depolarization via the mitochondrial permeability transition mechanism and loss of cell viability [5]. The main purpose of this study was to gain further insight into the mechanisms causing death in mtAQP8-knockdown HepG2 cells.

Mitochondrial permeability transition, a non-selective inner membrane permeabilization, may proceed necrotic and apoptotic cell death [13]. The induction of mitochondrial permeability transition may lead to the osmotic swelling of the mitochondrial matrix, rupture of the outer mitochondrial membrane, and the release of intermembrane space proteins to cytosol, including the apoptogenic factor, cytochrome c [14]. As shown in Fig. 1, the lack of release of mitochondrial cytochrome c into the cytosol indicates that although the mitochondrial permeability transition pore was induced and the mitochondrial function impaired [5], the permeability of the outer mitochondrial membrane was not significantly altered. The mitochondrial permeability transition pore may open transiently and the resulting mitochondrial swelling might not suffice to cause cytochrome c release and activation of the intrinsic mitochondrial apoptotic pathway, as previously described in non-hepatic cells [15, 16].

A feature of the early stages of apoptosis is the translocation of phosphatidylserine from the inner to the outer leaflet of the plasma membrane where it can then be detected using Annexin V in flow cytometry studies. The lack of either annexin V staining or cells undergoing chromatin fragmentation or condensation confirmed a non-apoptotic type of death (see Figs. 2c and 3).

Together, previous [5] and present data favor necrosis as the mode of death in mtAQP8-knockdown HepG2 cells. Thus, the loss of structural integrity of the plasma membrane, a hallmark of necrosis, was revealed by the LDH leakage and trypan blue exclusion tests [5], and most importantly, by flow cytometry with propidium iodide staining (Fig. 3). Necrotic death was also supported upon finding nuclear delocalization followed by increased extracellular release of HMGB-1 (Fig. 4) and reduced ATP levels in mtAQP8-knockdown HepG2 cells [5].

The knockdown of mtAQP8 also induced necrotic death in another human hepatoma cell line, i.e., HuH-7 (Table 1 and Results). Interestingly, mtAQP8 silencing did not induce loss of viability in either normal rat hepatocytes [17] or in the non-neoplastic human cell lines, renal HK-2 [18] and HeLa-derivative Chang cells (data not shown). Thus, hepatoma cells might be particularly susceptible to a defective expression of mtAQP8.

In mtAQP8-knockdown HepG2 cells mitochondrial ROS accumulation and loss of viability could be prevented by the mitochondria-targeted antioxidant MitoTempol [5]. Thus it is conceivable that a disparity in mitochondrial antioxidant defenses may explain the observed differential susceptibility among mtAQP8-knockdown cells. Further studies are required to understand the precise mechanisms that actually cause differential death of mtAQP8-knockdown cells.

In conclusion, our data suggest that mtAQP8 knockdown induces non-apoptotic, likely necrotic, death in neoplastic hepatic cells, a finding that might be relevant to therapeutic strategies against hepatoma cells.

Acknowledgments This work was supported by Grant PICT 0946 (R.A. Marinelli) from Agencia Nacional de Promoción Científica y Tecnológica.

Conflict of interest The authors declare that there is no conflict of interest.

References

1. Bienert GP, Møller AL, Kristiansen KA, Schulz A, Møller IM, Schjoerring JK, Jahn TP (2007) Specific aquaporins facilitate the diffusion of hydrogen peroxide across membranes. J Biol Chem 282:1183–1192

2. Miller EW, Dickinson BC, Chang CJ (2010) Aquaporin-3 mediates hydrogen peroxide uptake to regulate downstream intracellular signaling. Proc Natl Acad Sci USA 107:15681–15686
3. Calamita G, Ferri D, Gena P, Liquori GE, Cavalier A, Thomas D, Svelto M (2005) The inner mitochondrial membrane has aquaporin-8 water channels and is highly permeable to water. J Biol Chem 280:17149–17153
4. Ferri D, Mazzone A, Liquori GE, Cassano G, Svelto M, Calamita G (2003) Ontogeny, distribution, and possible functional implications of an unusual aquaporin, AQP8, in mouse liver. Hepatology 38:947–957
5. Marchissio MJ, Francés DEA, Carnovale CE, Marinelli RA (2012) Mitochondrial aquaporin-8 knockdown in human hepatoma HepG2 cells causes ROS-induced mitochondrial depolarization and loss of viability. Toxicol Appl Pharmacol 264:246–254
6. Elbashir SM, Harborth J, Lendeckel W, Yalcin A, Weber K, Tuschl T (2001) Duplexes of 21-nucleotide RNAs which mediate RNA interference in cultured mammalian cells. Nature 411:494–498
7. Ragan CI, Wilson MT, Darley-Usmar VM, Lowe PN (1987) Subfractionation of mitochondria and isolation of the proteins of oxidative phosphorylation. In: Darley-Usmar VM, Rickwood D, Wilson MT (eds) Mitochondria: a critical approach. IRL Press, Oxford, pp 79–112
8. Lowry OH, Rosebrough NJ, Farr AL, Randall RJ (1951) Protein measurement with the Folin phenol reagent. J Biol Chem 193: 265–275
9. Rasband WS (1997–2011) ImageJ. US National Institutes of Health, Bethesda, Maryland, USA (http://imagej.nih.gov/ij/)
10. Bustin M (1999) Regulation of DNA-dependent activities by the functional motifs of the high-mobility-group chromosomal proteins. Mol Cell Biol 19:5237–5246
11. Scaffidi P, Misteli T, Bianchi ME (2002) Release of chromatin protein HMGB1 by necrotic cells triggers inflammation. Nature 418:191–195
12. Vaseva AV, Marchenko ND, Ji K, Tsirka SE, Holzmann S, Moll UM (2012) p53 opens the mitochondrial permeability transition pore to trigger necrosis. Cell 149:1536–1548
13. Kinnally KW, Peixoto PM, Ryu SY, Dejean LM (2011) Is mPTP the gatekeeper for necrosis, apoptosis, or both? Biochim Biophys Acta 1813:616–622
14. Custodio JBA, Cardoso CMP, Almeida LM (2002) Thiol protecting agents and antioxidants inhibit the mitochondrial permeability transition promoted by etoposide: implications in the prevention of etoposide-induced apoptosis. Chem Biol Interact 140:169–184
15. Lim MLR, Minamikawa T, Nagley P (2001) The protonophore CCCP induces mitochondrial permeability transition without cytochrome c release in human osteosarcoma cells. FEBS Lett 503:69–74
16. Vande Velde C, Cizeau J, Dubik D, Alimonti J, Brown T, Israels S, Hakem R, Greenberg AH (2000) BNIP3 and genetic control of necrosis-like cell death through the mitochondrial permeability transition pore. Mol Cell Biol 20:5454–5468
17. Soria LR, Marrone J, Calamita G, Marinelli RA (2013) Ammonia detoxification via ureagenesis in rat hepatocytes involves mitochondrial aquaporin-8 channels. Hepatology 57:2061–2071
18. Molinas SM, Trumper L, Marinelli RA (2012) Mitochondrial aquaporin-8 in renal proximal tubule cells: evidence for a role in the response to metabolic acidosis. Am J Physiol Renal Physiol 303:F458–F466